Article

Microstructure and Mechanical Properties of Ti6Al4V Alloy Modified and Reinforced by In Situ Ti$_5$Si$_3$/Ti Composite Ribbon Inoculants

Nuo Li, Chunxiang Cui *, Shuangjin Liu, Shuiqing Liu, Sen Cui and Qian Wang

Key Laboratory for New Type of Functional Materials in Hebei Province,
School of Materials Science and Engineering, Hebei University of Technology, Tianjin 300130, China;
ln0713@126.com (N.L.); lshjin1977@126.com (S.L.); liushuiqing0824@126.com (S.L.); cuisen0624@126.com (S.C.);
wangqian296@163.com (Q.W.)
* Correspondence: hutcui@hebut.edu.cn; Tel.: +86-22-2656-4125; Fax: +86-22-6020-4125

Abstract: This paper deals with a novel fabrication method (a vacuum rapid solidification technique) to prepare in situ Ti$_5$Si$_3$/Ti composite ribbon as inoculants to modify Ti6Al4V alloy to obtain titanium matrix composites (TMCs). Microstructure and morphology observations showed that the grain size of the TMCs was refined as the volume fraction of inoculants increased. The grain size of the TMCs can be refined from a grade of 650 μm to about 110 μm with a very small refiner adding ratio of 0.6% in weight. Thereafter, the mechanical properties of the TMCs, including their tensile strength, microhardness, impact properties, and resistant properties were improved obviously by adding the ribbon inoculants. The excellent grain refining and reinforcement effect can be attributed to the nano-sized Ti$_5$Si$_3$ refiner particles distributed homogeneously in the matrix, the well-banded particle/matrix interface, and the good wettability between the Ti$_5$Si$_3$ particles in inoculants and the Ti6Al4V alloy melt, which are benefit for the heterogeneous nucleation of the TMCs during solidification.

Keywords: grain refinement; inoculant; titanium alloy; rapid solidification; heterogeneous nucleation; mechanical characterization

1. Introduction

Grain refinement by the addition of inoculants is acknowledged as an effective route to prodigiously improve the mechanical properties of cast metal, and is considered to be an economical industrial technology due to the very small adding amount of inoculants with a great grain refinement effect [1,2]. Over several decades, this technology has been widely used in metallurgical enterprises such as aluminum alloys [3–5], magnesium alloy [6], and steel materials [7]. Meanwhile, different kinds of ceramic particles, such as TiC [8,9], SiC [10], and TiB$_2$ [11,12], have been used as the active components of inoculants, which serve as substrates for heterogeneous nucleation. However, up to now, the studies related to titanium alloys refined by inoculants are still growing, and the exact grain refinement mechanism is unclear because of the complex solidification process, which limits its application. Therefore, the development of effective inoculants refining in titanium alloys and its related techniques have an application prospect and realistic significance.

Titanium matrix composites (TMCs) are widely used as a new type of promising engineering material, due to their high specific strength, low density, excellent corrosion behavior, specific modulus at high temperatures, and attractive fracture-related properties [13,14]. Because of these advantageous properties, TMCs are extensively used in the aerospace industry, petrochemical engineering, biomedical engineering, power generation, and other fields [15,16]. Recently, TMCs have been actively investigated

in order to improve their comprehensive mechanical properties [14,17,18]. The composite fabrication technology to introduce the hard and stiff particulate reinforcements to a Ti alloy matrix has proved to be an effective approach to increase the strength and hardness of the Ti matrix composites [19–21]. As is well known, many theoretical and experimental reports have proved that decreasing the sizes of the reinforcing ceramic particulates can lead to a significant improvement in the mechanical performance of TMCs.

However, there are some problems that need to be solved in the inoculation technology, such as the agglomerate of the particles in the Ti matrix melt, the large size of the adding particles, and a non-favorable wettability between the particles and the melt. For these reasons, the in situ method is utilized for the preparation of the composite inoculants that are Ti-rich and particle-contained, due to their advantages of a cleaner particle-matrix interface and the high purity of the products, while the Ti-rich composite inoculates can improve the wettability between the inoculants and the titanium alloy melt. Therefore, the idea to fabricate the TMCs reinforced by the in situ particulates as the inoculants to refine a titanium alloy matrix may help to overcome the above problems, and improve the comprehensive mechanical properties of titanium alloys used commonly in industry. Adding the composite inoculants into the titanium alloys can not only refine the grain size, but also introduce ceramic particulates to reinforce the strength of the titanium alloys. In this study, a new type of in situ Ti_5Si_3/Ti composite ribbon inoculants have been successfully developed; also, its refining and nano-particulate reinforcing effect on Ti6Al4V alloys are investigated in this paper. Adding the Ti_5Si_3/Ti composite inoculants ribbons into the melt of titanium alloys could significantly refine the grain size of the titanium alloys by providing many tiny nano-Ti_5Si_3 particulates as the heterogeneous nucleation cores to increase the heterogeneous nucleation rate. Meanwhile, the introduced nano-Ti_5Si_3 particulates could be used as strengthening particles to effectively improve the strength and ductility of the final TMC product. The test results will offer some new guidance to the fabrication, investigation, and application of titanium alloys and TMCs, and even more to the other metal matrix composites.

2. Materials and Methods

Commercial pure titanium (99.99 wt % in purity) and Ti6Al4V alloy was chosen as the matrix alloy. Also, commercially pure Si (99.9 wt % in purity) was used as the raw material to react with the Ti matrix to prepare the Ti_5Si_3/Ti composite inoculants. The reactants were mixed with the ratio of Ti–8.3 Si (in wt %) that is close to the eutectic composition, and melted in a non-consumable vacuum arc melting furnace under a high purity argon atmosphere at a positive pressure of 0.5 MPa to prepare Ti–Si intermediate alloy ingots. The schematic of the electric arc melting device is shown in Figure 1a. Each ingot was turned over and remelted six times, and the reaction times for each sample were kept to 120 s to ensure homogeneous chemical composition and sufficient in situ reaction time. Then, the alloy ingot was rapidly quenched by a melt-spinning process to form the in situ Ti_5Si_3/Ti composite ribbon inoculants. The schematic of the electric melt-spinning device is shown in Figure 1b. The experiments on the effect of grain refinement were carried out by adding the inoculants into a Ti6Al4V alloy during casting in a vacuum induction levitation suspended furnace. In order to compare the titanium and Ti6Al4V alloys, their preparation was carried out in a similar way. The specimens used for morphology and microstructure observations were cut from the middle part of the prepared materials, and mechanically polished with SiC paper and Al_2O_3 particles with water, then etched with the Kroll's reagent (composition: 1–3 mL HF, 2–6 mL HNO_3, and 100 mL H_2O).

The phase identification of the specimens was investigated via a Philips X' Pert BMP X-ray diffraction (XRD, Royal Dutch Philips Electronics Ltd., Amsterdam, The Netherlands) with Cu Kα radiation. Philips XL 30 TMP scanning electron microscope (SEM Royal Dutch Philips Electronics Ltd., Amsterdam, The Netherlands) with EDAX energy-dispersive spectrometry (EDS) was used to observe and analyze the microstructure and compositions of the specimens. The optical microstructure of each sample was observed by BX41M Olympus optical microscope (Olympus Corporation, Tokyo, Japan). A JEOL 2000FX High-Resolution Transmission Electron Microscope (HRTEM, Shimadzu

Corporation, Kyoto, Japan) was used to observe the microstructure of the reinforced phase and Ti alloy matrix. The standard-sized tensile specimens were prepared for the test of mechanical properties. The microhardness was determined via a HR-150A type Rockwell Hardness Tester (Optical inctrument factory, Shanghai, China). The test of impact properties was investigated via a JB-300B type pendulum impact tester (Fangyuan Experimental solutions co. Ltd., Jinan, China), and the abrasion resistance properties were determined via an M-200 type friction and wear tester (Beijing zhongna Equipment co. Ltd., Beijing, China).
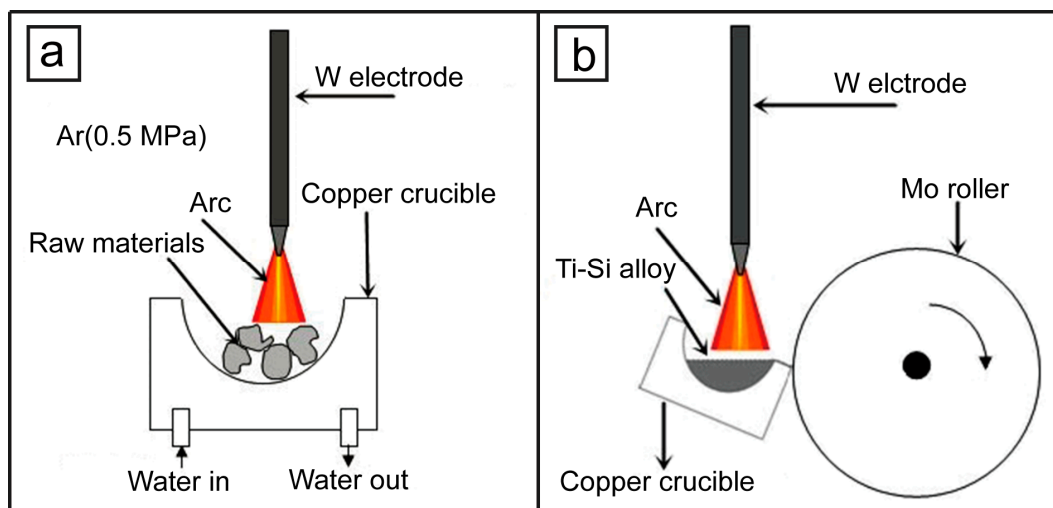

Figure 1. The schematic of experimental devices: (**a**) electric arc melting device; (**b**) melt-spinning device.

3. Results

3.1. The Design and Formation Mechanism of Ti_5Si_3/Ti Composite Ribbon Inoculants Synthesized by In Situ Reaction

Due to the lowest solidification temperature of the eutectic composition alloy, the alloy in its liquid state has higher superheat to a certain degree, delaying solidification. Because the solidification time can be extended, the fluidity usually facilitates a subsequent inoculate refinement. In view of the above reasons, we designed the nominal composition of the master alloy with Ti–8.3Si (wt %) as eutectic composition in this paper.

According to the Ti–Si binary phase diagram shown in Figure 2, when solidification takes place at the eutectic composition of Ti–8.3Si (wt %), the following reactions occur: (1) a eutectic reaction in 1330 °C: L (Ti, Si) → Ti + Ti_5Si_3; (2) a peritectoid reaction in 1170 °C: β-Ti + Ti_5Si_3 → Ti_3Si; and (3) a eutectoid reaction in 865 °C: β-Ti → α-Ti + Ti_3Si. In the above reaction equations, the Ti_3Si is a transitional phase that can be obtained under the condition of heat preservation of 120 h at 1200 °C or heat preservation of 115 h at 1000 °C, in which it has gone through the peritectiod reaction and eutectoid reaction [22]. In this paper, Ti_5Si_3 is the final reaction product rather than Ti_3Si, while the peritectiod transformation cannot occur due to the cooling condition of the casting process being too fast.

The X-ray diffraction (XRD) pattern of mater alloys and inoculant ribbons are shown in Figure 3. The α-Ti and Ti_5Si_3 diffraction peaks can be observed in the XRD pattern of the Ti–Si mater alloys (shown in Figure 3a) without other impurity peaks existing. Figure 3b shows the SEM images of the Ti–Si master alloys. The SEM morphology presents a typical eutectic microstructure with a large number of bright white precipitate Ti_5Si_3 phases distributed homogeneously in the dark grey α-Ti matrix, and the result agrees well with that in the XRD result in Figure 3a. Figure 3d shows the SEM morphology of the inoculants ribbons. It can be seen that the microstructures of the ribbons are refined obviously after the melt-spinning treatment in contrast to the master alloys, which may be attributed to the too rapid cooling rate of the melt-spinning. The XRD pattern of the ribbon inoculants (shown in Figure 3c) only contains

α-Ti and Ti$_5$Si$_3$ without other impurity peaks existing. This suggests that melt-spinning is an effective method to refine an inoculant's microstructure without affecting its phase composition.

Figure 4a shows the microstructures of the in situ Ti$_5$Si$_3$/Ti composite inoculant ribbon. It indicates that inerratic isometric-shaped cellular structures are distributed homogeneously in the inoculants ribbon after melt-spinning. The mean particle size of the cell is about 70–90 nm in a uniform structure. The boundary of the cellular structures (region B) is the Si-rich region, while the core of the cellular structures (region A) represents a region of low Si content. Because the melt-spinning is a process with short heating time and rapid heating rate, dissolving Si from the Ti$_5$Si$_3$ phase has no time to diffuse in the rapid cooling process to form a supersaturated solid solution in a certain region of the Ti-matrix. The schematic diagram of the formation process of the cellular interface is shown in Figure 4d.
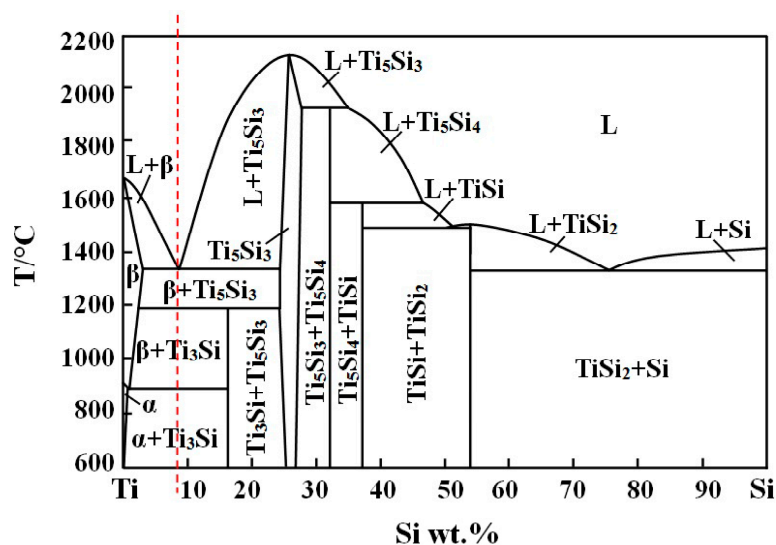
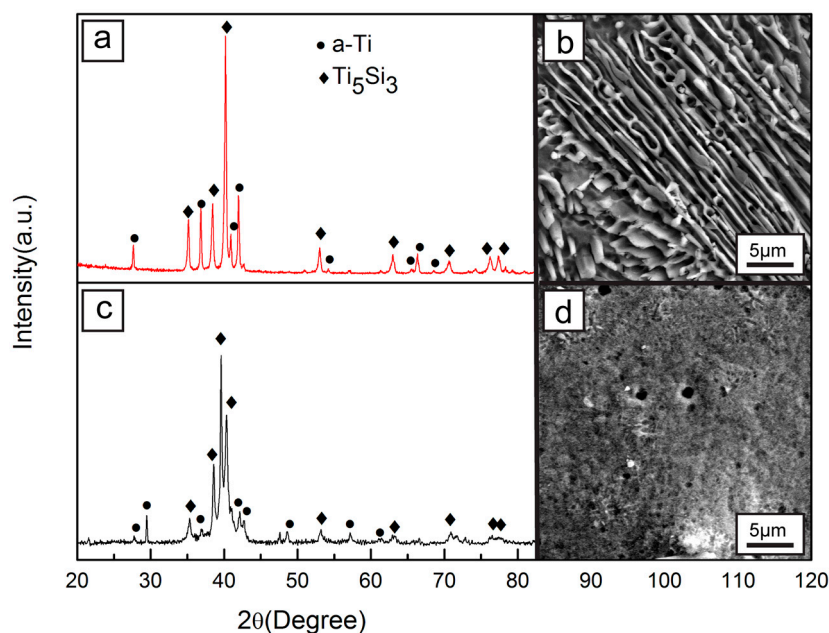

Figure 2. The Ti–Si binary phase diagram.

Figure 3. X-ray diffraction (XRD) patterns and scanning electron microscope (SEM) images of the in situ Ti$_5$Si$_3$/Ti composite inoculants: (**a**) XRD patterns of Ti–Si master alloy; (**b**) SEM image of Ti–Si master alloy; (**c**) XRD patterns of inoculants ribbons; (**d**) SEM image of inoculants ribbons.
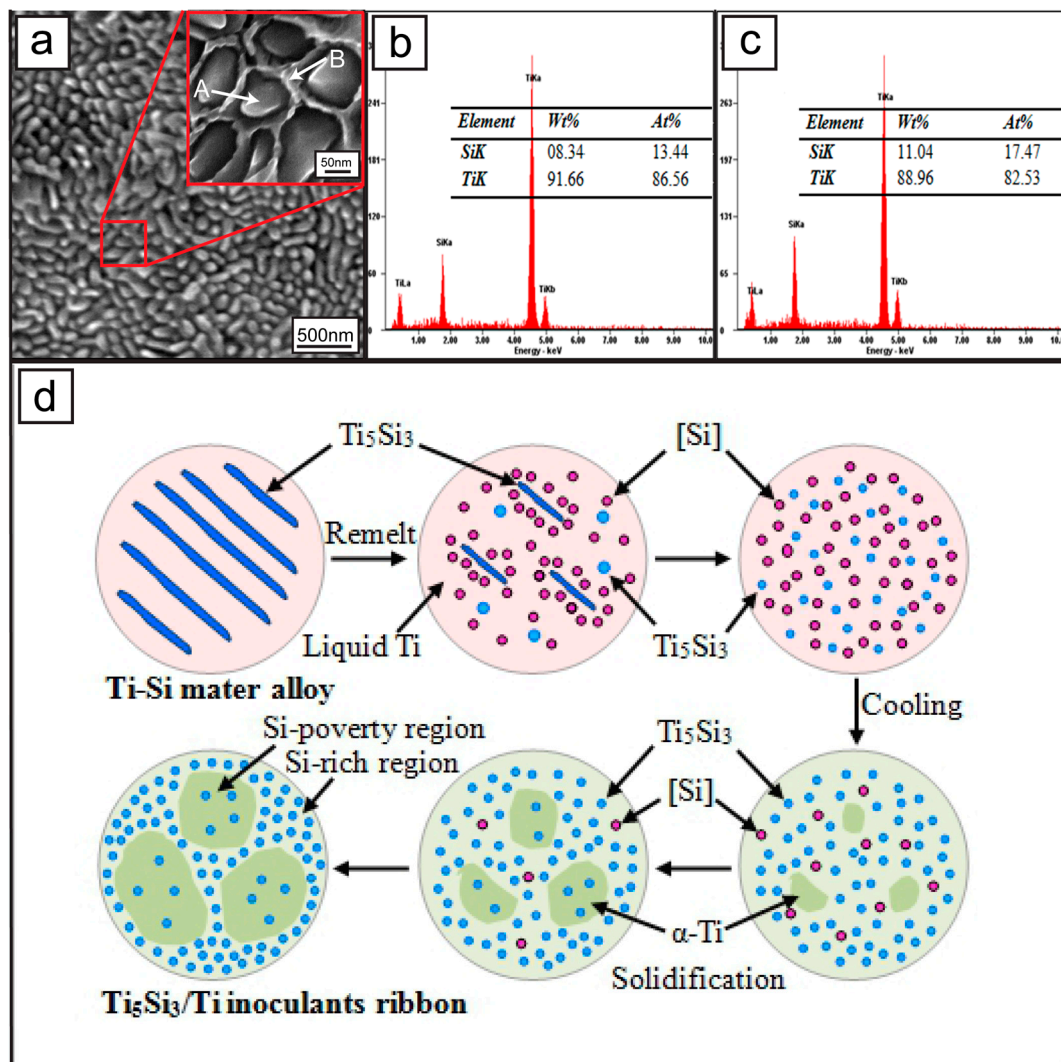
Figure 4. Microstructures of the in situ Ti_5Si_3/Ti composite inoculants and the schematic diagram of its formation process: (**a**) microstructures; (**b**) energy-dispersive spectrometry (EDS) result of point A; (**c**) EDS result of point B; (**d**) the schematic diagram of the cellular formation.

Due to solidification in the Ti–Si alloy occurring in a temperature range from liquid temperature to room temperature, the equilibrium compositions of the liquid phase and the solid phase in the two phase regions are different. Therefore, the Equilibrium partition coefficient can be indicated as:

$$k_{0\ Ti-Si} = \frac{C_{S\ Ti-Si}}{C_{L\ Ti-Si}} \tag{1}$$

where $C_{S\ Ti-Si}$ is the equilibrium composition of the solid phase, and $C_{L\ Ti-Si}$ is the equilibrium composition of the liquid phase. In the solidification process of the Ti–Si alloy, the solute atoms are redistributed and enriched in the liquid, especially in the front of the interface. So, the solidification point is lower with the result of the heat's dissipation, and there exists a temperature gradient in the liquid phase resulting in a constitutional supercooling. When the Ti–Si alloy solidifies, the solute atoms are released on the front of the solid/liquid interface ($k_0 < 1$). So, besides the influence of the heat flux, the solid growth is also affected by the diffusion of the solute atoms playing a main role in the interface morphology. Due to the rough interface of the metal, the crystal morphology of the pure metal is affected by the temperature gradient. However, for solid solution alloys, beside the influence of the temperature gradient, the crystal morphology is affected by constitutional supercooling more seriously.

Under the negative temperature gradient, the crystal morphology of the solid solution tends to grow into dendritic-shape that is the same as pure metal, while under the positive temperature gradient, the constitutional supercooling formed by enrichment of the solute elements at the forefront of the solid-liquid interface will produce a great impact on the crystal morphology of the solid solution alloys. Under a certain temperature gradient, there are smaller constitutional supercooling regions existing in the front of the solid-liquid interface, so the several tiny protrusions on the smooth interface can grow into the supercooling regions. The protrusions grow not only along the perpendicular direction to the solid-liquid interface, but also in the other direction to vent the solute into the surrounding environment. Because the diffraction condition of the solute atoms at the top of the protrusions is better than that in the other direction, it is beneficial to diffusion from the solid-liquid interface to the liquid. As a result, the solute concentrations of the grooves between the adjacent protrusions increase more seriously than those on the top, which leads to solute enrichment in the grooves. At the same time, the equilibrium crystallization temperature of the liquid decreased with the increase of solute concentration. Therefore, the equilibrium crystallization temperature of the enriched grooves with solute atoms becomes lower and the supercooling degree becomes smaller, which makes the growth speed of the protrusions in the grooves slower than that on the top parts and the grooves more deepened. As the constituent supercooling on the front of the interface increases, the protrusions on the interface increase too, connecting and forming regular networks. Under a certain condition, the interface reaches a steady state eventually, then crystal growth process is accompanied by the movement of an uneven stable interface to the liquid at a constant speed, forming a cellular structure eventually.

After the melt-spinning treatment, the inoculant ribbons show a microstructure evolution, which has more uniform cores to provide heterogeneous nucleation. So, the in situ Ti_5Si_3/Ti composite inoculant is expected to be a new type of effective inoculant to refine titanium alloys and TMCs with a favorable melt-spinning processing step.

3.2. Refinement Effect of Titanium Matrix Composites (TMCs)

To examine the refining effect of the in situ Ti_5Si_3/Ti composite ribbon inoculants, pure titanium was used as a reference to check the different added fractions of inoculants. Figure 5 shows the metallographic microstructure of Ti and Ti6Al4V alloys unmodified and modified by in situ Ti_5Si_3/Ti composite ribbon inoculants with different weight percentages. Generally, the inoculants present a refining effect. There is a trend that the refining effect becomes more effective as the adding fraction of the inoculants is increased. Figure 6 shows the optical microstructure of the TMCs. It is indicated in Figure 6 that the grain size of the TMC sample is significantly decreased with the addition of the inoculants. It shows that the grain size of TMCs without inoculation is about 650 μm. Interestingly, by adding 0.6 wt % Ti_5Si_3/Ti composite ribbon inoculants, this grain size is refined and transformed into small grains with a size of about 110 μm. Such a small adding fraction with such a significant refining effect suggests that the in situ Ti_5Si_3/Ti composite ribbons are one type of efficient inoculant to modify a Ti6Al4V alloy melt. In addition, the microstructure of Ti6Al4V unmodified is a mixture of a plate-like acicular alpha and beta phase with large beta grains (shown in Figure 6a). By adding 0.2 wt % Ti_5Si_3/Ti composite ribbon inoculants, the acicular-like structure from the supersaturated alpha phase is turned into finer grains with the decreasing of grain size. With the increasing of the inoculant content, the size of the acicular structure becomes even smaller. But when adding 0.6 wt % inoculant, a small amount of impurity is present at the boundary of the tiny grains, and little tiny holes and defects also emerge in the matrix (shown in the rectangular regions of Figure 6d).
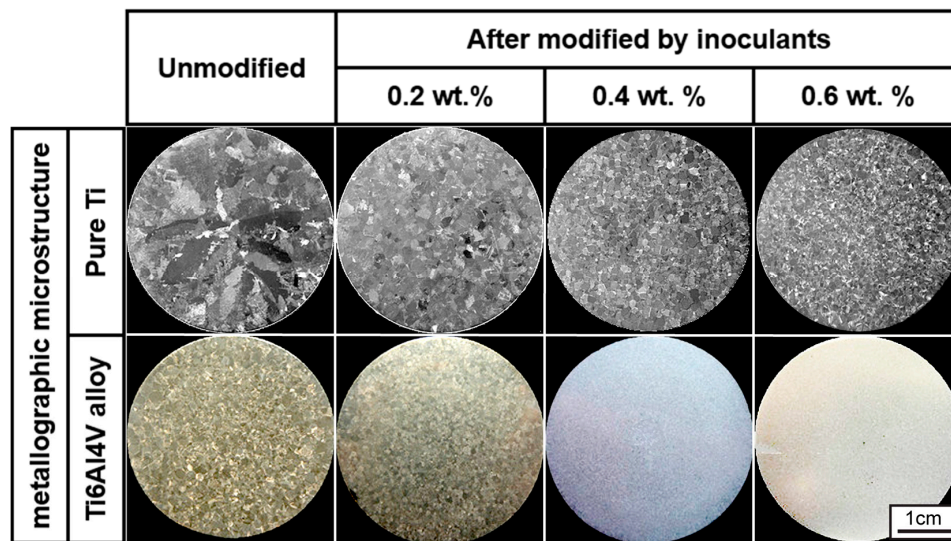
Figure 5. The metallographic microstructure of pure Ti and Ti6Al4V alloys unmodified and modified by in situ Ti$_5$Si$_3$/Ti composite ribbon inoculants with different weight percentages.
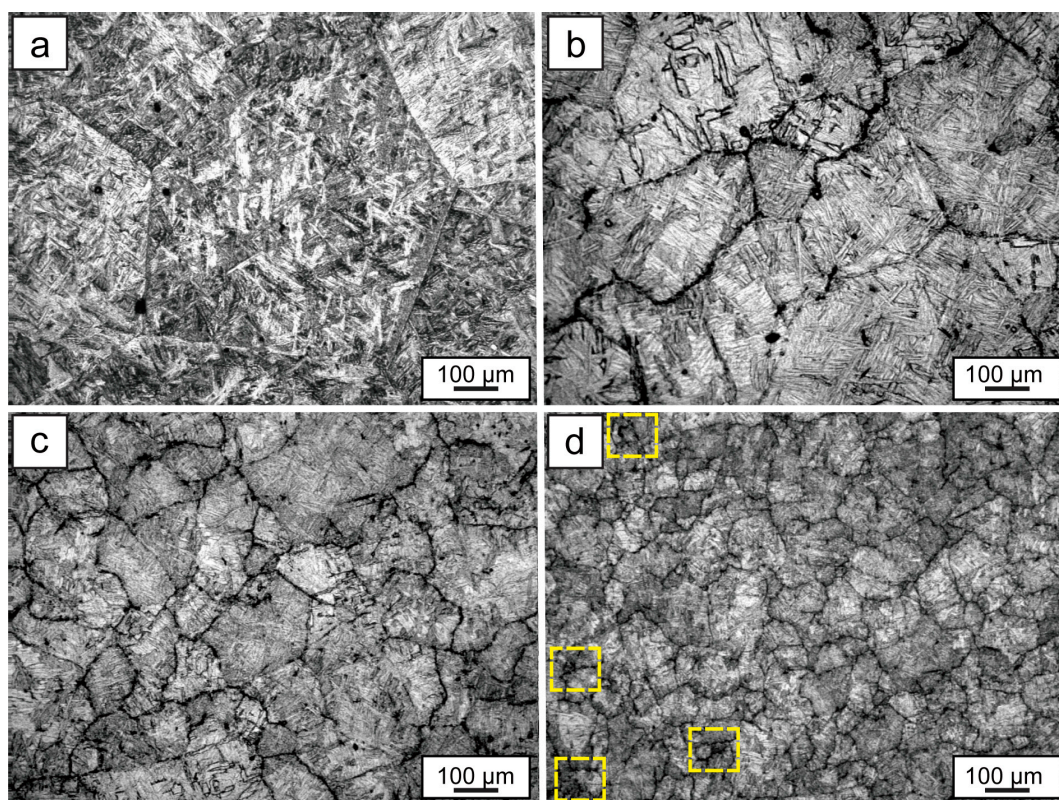

Figure 6. The metallographic microstructure of titanium matrix composites (TMCs) unmodified and modified by in situ Ti$_5$Si$_3$/Ti composite ribbon inoculants with different weight percentages: (**a**) TMCs unmodified; (**b**) TMCs modified with 0.2 wt. % inoculant; (**c**) TMCs modified with 0.4 wt. % inoculant; (**d**) TMCs modified with 0.6 wt. % inoculant.

Figure 7 shows transmission electron microscope (TEM) images of the TMCs in a refined and reinforced condition by in situ Ti$_5$Si$_3$/Ti composite ribbon inoculants. The Ti$_5$Si$_3$ particle, which can be observed by transmission electron microscope, is too small to be seen by scanning electron microscope. One can see clearly that the Ti$_5$Si$_3$ particles with a size of less than 10 nm are embedded in the matrix

homogeneously. It is necessary for us to point out that the nano-scale Ti_5Si_3 particles exist inside the Ti6Al4V alloy grain, which means that the nano-Ti_5Si_3 particles can exist in a stable state in the melt and act as cores for heterogeneous nucleation. At the same time, the nano-scale Ti_5Si_3 particles greatly contribute to the refining and reinforcement of Ti6Al4V alloy. To further confirm the morphology and size of the Ti_5Si_3 particles, the HRTEM image is shown in Figure 7c. The Fast Fourier transform (FFT) analysis in Figure 7d corresponds to the [110] zone axis of the hexagonal Ti_5Si_3 structure, so it is confirmed that this is the major phase in the beam spot area.
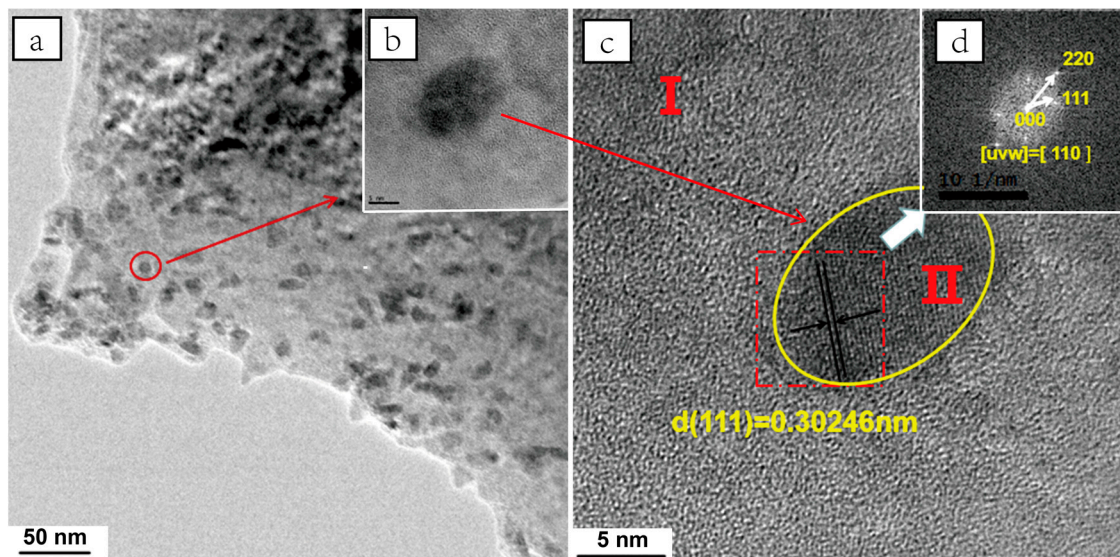

Figure 7. The transmission electron microscope (TEM) images and Fast Fourier transform (FFT) analysis of TMCs refined and reinforced by in situ Ti_5Si_3/Ti composite ribbon inoculants: (**a**) TEM image of TMCs; (**b**) TEM image of the Ti_5Si_3 particle in TMCs; (**c**) HRTEM image of nano-Ti_5Si_3 particle microstructure; (**d**) FFT analysis in the selected area II in Figure 7c.

The electron diffraction imaging is shown in Figure 8. Two groups of diffraction spots corresponding to Ti and Ti_5Si_3 can be observed in Figure 8b. The main phase corresponds to titanium, and the second phase is identified as a Ti_5Si_3 phase with a hexagonal crystal structure (a = 0.239 nm). There is no evidence of a clear orientation relationship between the Ti_5Si_3 phase and the surrounding Ti matrix. Therefore, it can be suggested that the particles shown in Figure 8a are Ti_5Si_3 phase that came from the addition of the in situ Ti_5Si_3/Ti composite ribbon inoculants.

The refining mechanism of inoculants can be explained from the following aspects. First of all, the good interface bonding is one of the factors that promote a refinement effect [23,24]. The homogeneously distributed nano-Ti_5Si_3 particles were directly formed in the Ti_5Si_3/Ti composite inoculants by the in situ reaction, thus the matrix/reinforcement interface is not only clean and taintless, but also these in situ particles have a good wettability and strong interface bonding with the matrix of TMCs that is attributed to the in situ Ti_5Si_3/Ti inoculants, which is itself a type of Ti_5Si_3 precipitate phase reinforced Ti matrix composite with a fine grain. When introducing an enhanced phase into the titanium alloys via the composite inoculants, the Ti matrix of the inoculants can be melted in the titanium alloy and the tiny reinforcing particles are distributed in the melt homogeneously, which ensures a good wettability between the reinforcing particles and matrix, thus leading to a desirable interface bonding. At the same time, the first-melted Ti matrix in the inoculant leads to the quantity of the crystal nuclei increasing, which can increase the number of short-range ordered clusters in a Ti6Al4V alloy melt. Furthermore, a small amount of silicon diffused into intervals of the short-range order in the Ti6Al4V melt. The combination of these two aspects increased the homogeneous nucleation of the Ti6Al4V alloy melt.
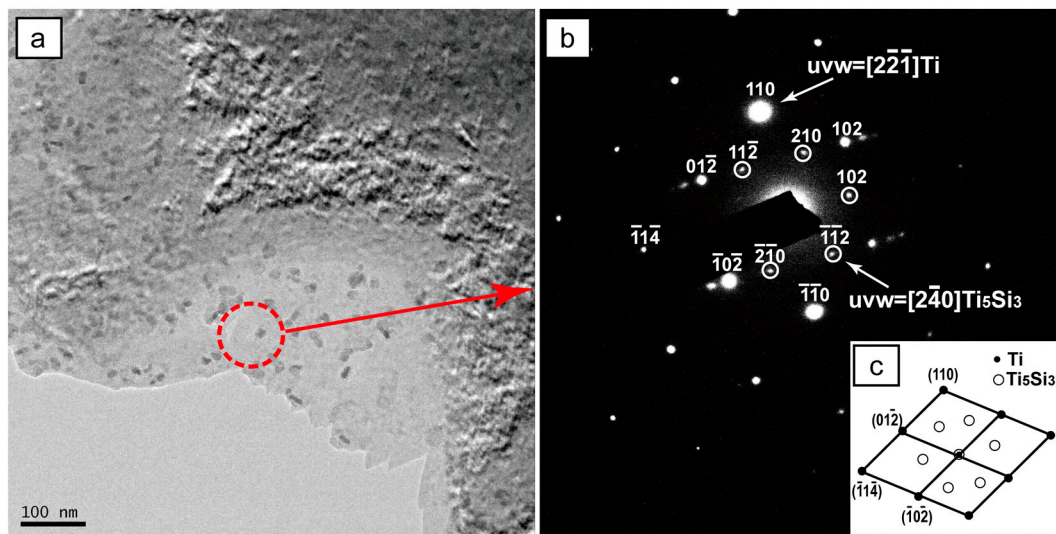
Figure 8. The TEM images and selected area electron diffraction (SAED) of TMCs refined and reinforced by in situ Ti_5Si_3/Ti composite ribbon inoculants: (**a**) TEM image of TMCS; (**b**) SAED in the zone A in Figure 8a; (**c**) the structure model of diffraction spots.

On the other hand, the tiny nano-Ti_5Si_3 reinforcing particles are homogeneously distributed in the TMCs matrix as shown in Figure 7a, indicating that their size is less than 10 nm. The generation of nano-sized reinforcing particles is mainly due to the previous melt-spun, which brings a great degree of supercooling through the huge cooling rate. With a constant silicon element content, the number and size of the reinforcing particles showed an inverse proportion. While the size of the reinforcing particles become smaller, the number of the nano-sized particles increased considerably, providing more cores for heterogeneous nucleation, and improving the nucleation rate and promoting heterogeneous nucleation. In addition, according to Stoke's Formula [25,26]:

$$u_t = \frac{2d_p^2(\rho_p - \rho)g}{9\eta} \tag{2}$$

where u_t is the sedimentation rate of the particles, d_p is the particle radius, g is acceleration of gravity, ρ_p is the particle density and η is the melt viscosity, it can be seen that the particle sedimentation rate is directly proportional to the particle radius. When the Ti_5Si_3 particle radius is decreased, the sedimentation rate is reduced, which is beneficial to the homogeneous distribution of the nano-Ti_5Si_3 reinforcing particles in the melt, and avoids the gravity segregation caused by the differences of density between the particles and the melt. Meanwhile, the time of the grain refining could be extended and the grain refining effect could be improved.

Finally, it is important to indicate that the heterogeneous nucleation of the titanium grain on the Ti_5Si_3 phases in the TMCs is playing a vital role in the grain refining. Owing to the nano-scale effect, the Ti_5Si_3 particles have high surface energy and a strong adsorption effect. So, the titanium grain can attach to the existing nano-Ti_5Si_3 crystal nucleus and nucleate in a smaller degree of supercooling due to the reduced nucleation interface energy. However, the good lattice mismatch between the reinforcing phase and the matrix phase plays a key role in the reduction of the interfacial energy. As we know, the typical structure of Ti6Al4V alloys is composed of a primary β-Ti phase and a laminar α-Ti phase. The α-Ti phase is precipitated during the β-α transformation. The α-Ti phase and β-Ti phase follow the specific orientation relationship: {0001}α//{110}β, <1120>α//<110>β. The different crystal lattice parameters are listed in Table 1. Obviously, the Ti_5Si_3 phase as well as the α-Ti phase belong to the hexagonal crystal system, owing the close-packed plane (0001) and a spacing of d0001 = 0.516 nm.

Generally, the mismatch degree of the close-packed plane can be expressed by the Turnbull–Vonnegut Formula [17]:

$$\delta = \frac{|a_s - a_n|}{a_n} \tag{3}$$

where a_s is the close-packed spacing of the parent phase, and a_n is the close-packed spacing of the precipitate phase. The smaller the degree of mismatch δ, the better the matrix and nucleation of crystal lattice matches and the smaller the change of energy causing the lattice mismatch, while the smaller interfacial energy makes the heterogeneous nucleation more likely to happen. According to the planar lattice mismatch theory by Bramfitt [27], the occurrence of nucleation particles that are the most effective with the mismatch of the two phases is less than 6%, so the Ti_5Si_3 phase can be used as the effective nucleating agent for the titanium alloy. Due to the same crystal system and the small mismatch between Ti_5Si_3 and α-Ti, the α-Ti tends to grow along the (0001) plane of Ti_5Si_3. As the content of Ti_5Si_3 reinforcement is increased, there would be more heterogeneous nuclei, leading to the refinement of α-Ti. When refined by Ti_5Si_3 particles, there would be more grain boundaries of α-Ti than in the β-Ti phase to heterogeneously nucleate. So, the nucleation rate of the β-Ti phase will be increased. Furthermore, the smaller sized α-Ti grain would restrain the growth space for the β-Ti phase, which could also cause a refining of β-Ti.

Table 1. Lattice parameters of different crystals.

Substance	Crystal System	Lattice Parameters		
		a/nm	b/nm	c/nm
Ti_5Si_3	Hexagonal (D88)	0.747	0.747	0.516
α-Ti	HCP	0.295	0.295	0.468
β-Ti	BCC	0.328	0.328	0.328

3.3. Mechanical Properties of TMCs

The mechanical properties of TMCs identified from the tensile tests are illustrated in Figure 9. Generally, the tensile strength of the TMCs was improved with the increase of inoculant content. However, in contrast, the elongation decreased with the increase of inoculant content. When the addition of in situ Ti_5Si_3/Ti composite inoculants reaches 0.4 wt %, the TMCs show the best mechanical properties of tensile strength, reaching 1105 MPa, which represents an increase of 12.6% compared to Ti6Al4V, where the elongation decreased by 13.1%. When increasing the inoculant content to 0.6 wt by adding 0.6 wt % Ti_5Si_3/Ti composite ribbon inoculants, the grain size is refined smaller. However, with an overdose of inoculants of 0.6 wt %, a small amount of impurity is present at the boundaries of the tiny grains, and little tiny holes also emerge in the matrix (shown in Figure 6d). The intermetallic compound coming from the inoculants attached at the grain boundary dissected the continuity of the substrate. So, the tensile strength decreased when adding 0.6 wt % inoculant.

The TMCs show the characteristics of brittle fracture, as shown in Figure 10, and with the increasing of the inoculant content the trend of the brittle fracture becomes more serious. There are some tearing ridges and a few dimples present in the matrix of the TMCs unmodified (shown in Figure 10a). After modification by adding 0.2 wt % inoculant, the dimples have disappeared and the river pattern appears in the fracture morphology, which shows the typical characteristics of a brittle fracture. With the increasing of inoculant content, the trend of the brittle fracture becomes more serious. When modified by 0.6 wt % inoculant, large cleavage steps appear in the fracture surface. Furthermore, we can see the tearing ridges become short and thick with the increasing of inoculant content. Because the formation of the tearing ridge is due to the intercrystalline fracture, the size of the grain is decreased with the inoculant content increased, which causes the tearing ridges to turn short and thick. These changing trends of the fracture morphology coincide with the results of the stress-strain curves from the tensile tests. The above two aspects suggest that the strength of the TMCs increased and their

toughness decreased by modification with inoculants. Considering the increase of tensile strength, we suggest that TMCs with an added 0.4 wt % inoculant have the optimal mechanical properties.
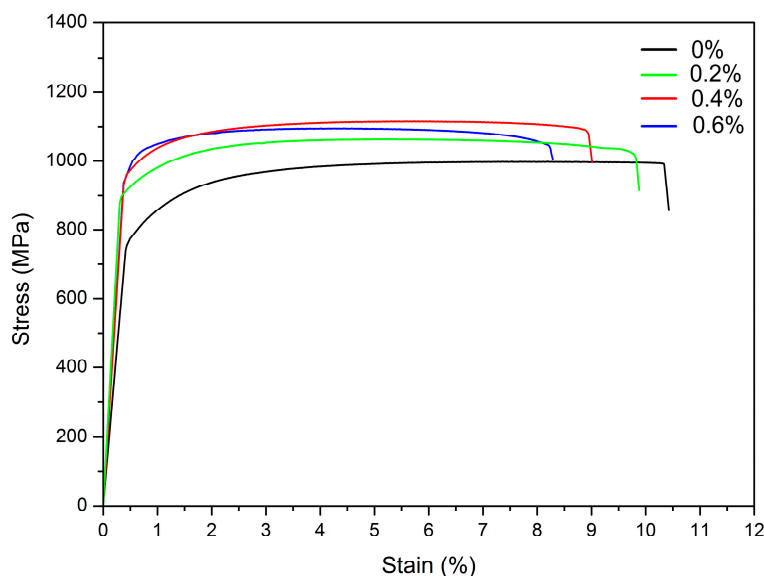

Figure 9. Stress-strain curves from tensile tests of Ti6Al4V alloy refined and reinforced with different weight fractions of ribbon inoculants.
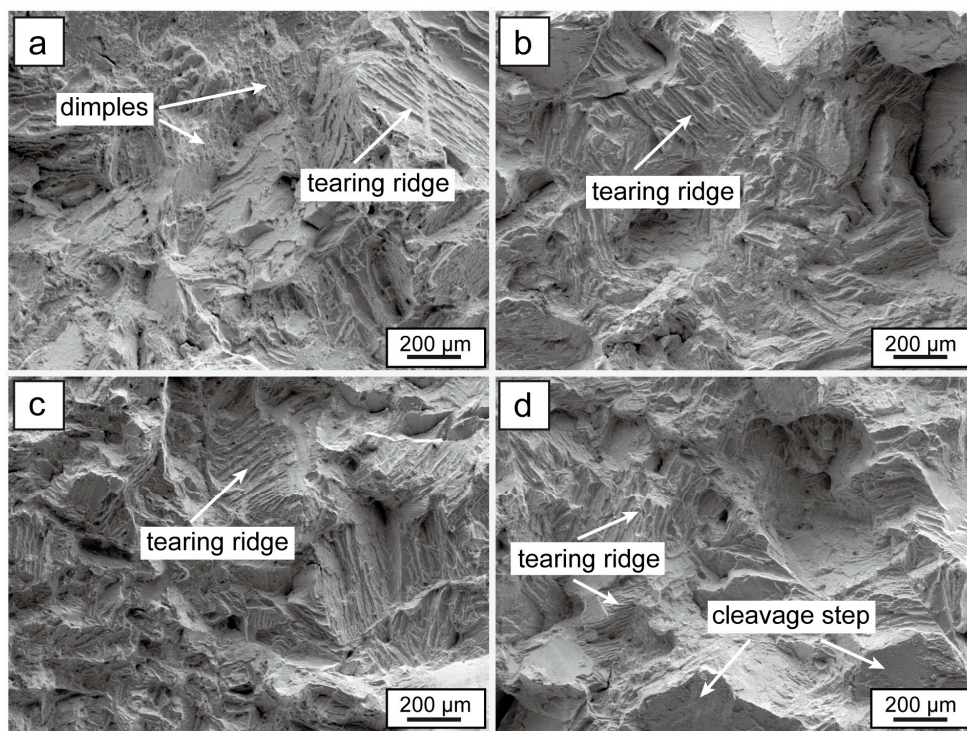

Figure 10. The SEM images of tensile fracture morphology for Ti6Al4V alloy modified and reinforced by Ti$_5$Si$_3$ composite ribbon inoculants: (**a**) Ti6Al4V alloy matrix; (**b**) TMCs modified by 0.2 wt % inoculants; (**c**) TMCs modified by 0.4 wt. % inoculants; (**d**) TMCs modified by 0.6 wt. % inoculants.

The improvement in mechanical properties of the TMCs can be explained from the interaction between the grain refining and the particle reinforcing effects. The reinforcing mechanism of the TMCs can be analyzed and summarized as follows: a fine-grain strengthening mechanism, a particle

strengthening mechanism, and a solution strengthening mechanism. For tensile strength, the first two increase levels of strength. The grain refinement is the result of the grain boundary being pinned to impede dislocation movement, while the particle reinforcement acts as a dispersion, strengthening that the nano-scale particles pin the motion of dislocations. Moreover, the strengthening of the TMCs enhanced with the reinforcement content can be explained by the Orowan strengthening mechanism, where critical shear stress results in the dislocation line by passing the reinforcement particles, expressed as:

$$\sigma_c = \frac{Gb}{2r} \tag{4}$$

where G is the shear modulus of the matrix, b is Buerger's vector, and r is the radius of the curvature of the dislocation line bending. The distance between the reinforcement particles $L = 2r$, so Equation (3) could be written as:

$$\sigma_c = \frac{Gb}{L}. \tag{5}$$

It is clearly seen from Equation (4) that with adding the content of the particles, the inoculant content of reinforcement increases the distance L. The solution strengthening, on the other hand, is composed of a primary β-Ti phase and a laminar α-Ti phase, while the alloying elements caused a lattice distortion and hinder the dislocation motion contributing to the improvement of the strengthening.

It is important to point out that the mechanical properties of the TMCs prepared by adding inoculant ribbons are more different from the TMCs prepared by adding Si powers to the Ti6Al4V alloy melt directly. As shown in Figure 11, the mechanical properties of tensile strength and elongation are superior. This result is consistent with previous results reported by Zhao et al. [17]. This is due to the homogeneous distribution of nano-scale Ti_5Si_3 reinforcement particles as described above (shown in Figure 8a). However, for the in situ synthesized TMCs, the reinforcement appeared segregated at the grain boundaries (shown in Figure 12b), which could be a serious reason for the decrease of the mechanical properties. Related studies [28] show that when the particle (acting as a core for heterogeneous nucleation) is less than 400 nm, the particles will be swallowed up into the interior of the matrix metal grain to result in an improved intracrystalline reinforcing effect. On the contrary, when the size of an in situ reinforcement particle is larger than 400 nm, it would be pushed to the grain boundary that not only does not have a reinforcement effect, but also lacerates the substrate reducing the mechanical properties.
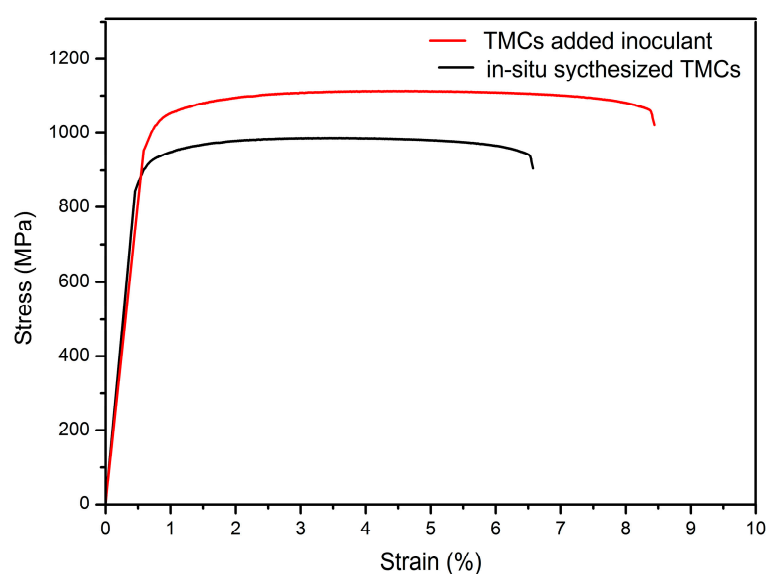

Figure 11. The stress-strain curves of TMCs modified and reinforced with 0.6 wt % inoculants and reinforcement prepared by different methods.
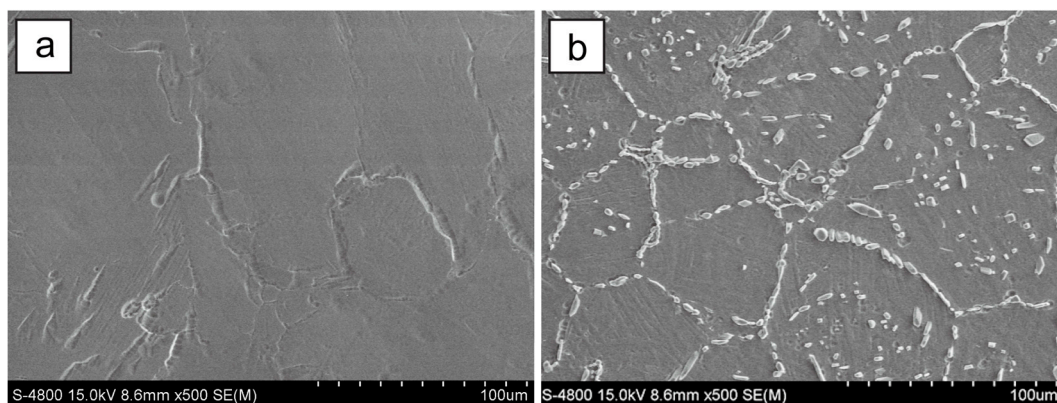
Figure 12. The SEM images of TMCs modified and reinforced with 0.6 wt % inoculants and reinforcement prepared by different methods: (**a**) TMCs prepared by adding ribbon inoculants; (**b**) in situ synthesized TMCs.

Figure 13 shows the result of the hardness test. For the TMCs, the microhardness values had a tendency to increase as the inoculate content increased. In particular, the mcirohardness of the alloys refined by adding the 0.6 wt % Ti_5Si_3/Ti composite inoculant has reached up to 113.2 HRB, which is improved 25.8% than that without inoculation. So, we can think that the optimization of the microstructure and the improvement of the comprehensive mechanical properties of TCMs are also benefited by the hard reinforcing particles and the refined grain size.
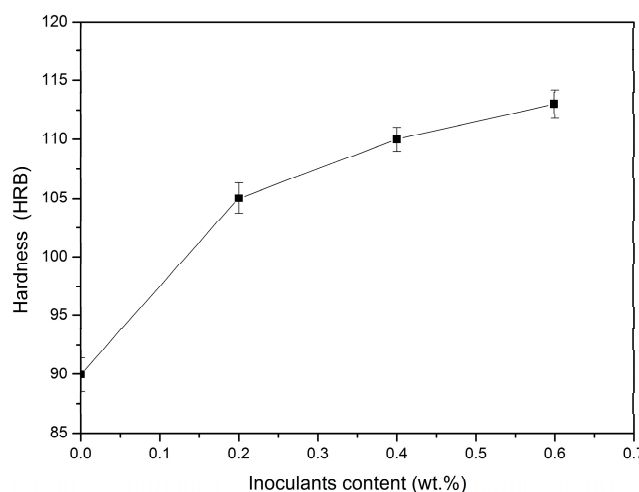

Figure 13. The hardness test result of the TMCs.

It can be seen from Figure 14 that the value of the impact toughness has a general trend of decrease with an increased weight fraction of inoculant. However, when the weight fraction of the inoculant is 0.2 wt %, the impact toughness is 28.1 J/cm^2, and in the SEM images of the impact fracture appear dimples and cleavage planes (shown in Figure 14b), which show the characteristics of cleavage fracture. When the weight fraction of inoculant is increased to 0.6 wt %, the impact toughness is reduced to 16.8 J/cm^2. The SEM images of the impact fracture present a rock candy shape feature (shown in Figure 14d), which suggests that the fracture mode has been turned into an intergranular fracture. Compared with the static tensile test, the embrittlement of the TMCs in the impact test occurs more seriously.

Figure 15 shows the friction and wearing test result of the TMCs. The values of weight loss percentage present a similar trend to that of the impact toughness in that the weight loss percentage is decreased as the reinforcement content is increased, which means that the wear-resisting property of

the TMCs improved. Figure 16 shows the SEM images of the wear surfaces. With the increase of the reinforcement content, a ploughed furrow appears and the spalled wear debris disappears gradually, which suggests that the friction and wear mechanism is abrasive wear instead of adhesive wear. The changing trends of the hardness, impact properties, and the wear resistance properties of the TMCs influenced by the inoculant content is consistent with the tensile properties of the TMCs.
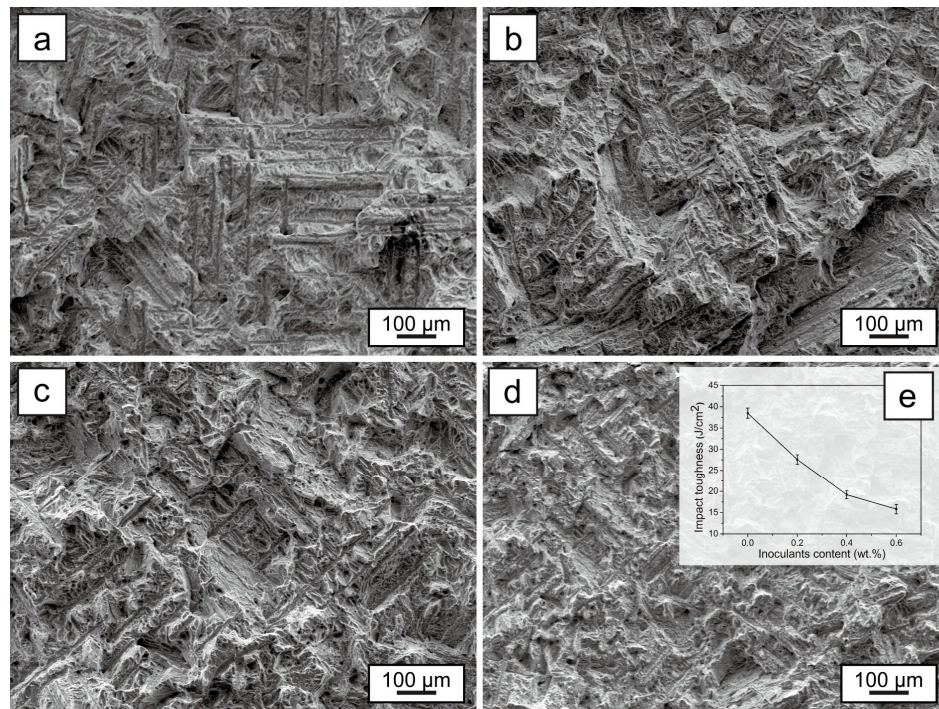

Figure 14. The impact test result of the TMCs: (**a**) the SEM image of the impact fracture of the TMCs unrefined; (**b**) the SEM image of the impact fracture of the TMCs refined by 0.2 wt % inoculants; (**c**) the SEM image of the impact fracture of the TMCs refined by 0.4 wt % inoculants; (**d**) the SEM image of the impact fracture of the TMCs refined by 0.6 wt % inoculants; (**e**) the impact toughness curve of the TMCs modified by inoculants with different weight fraction.
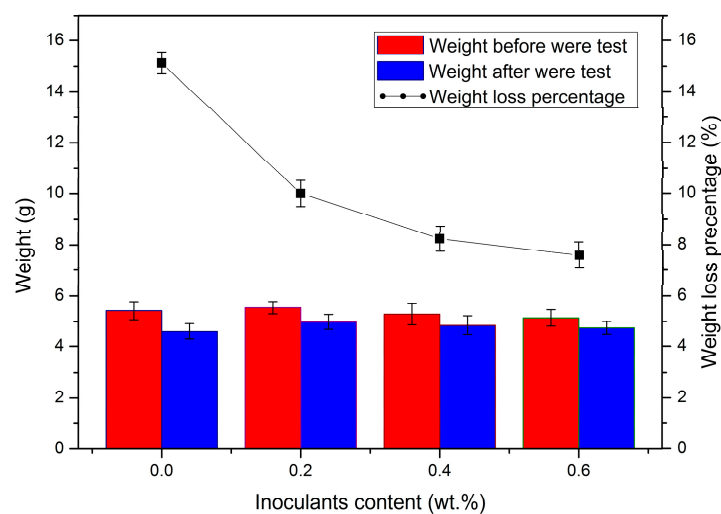

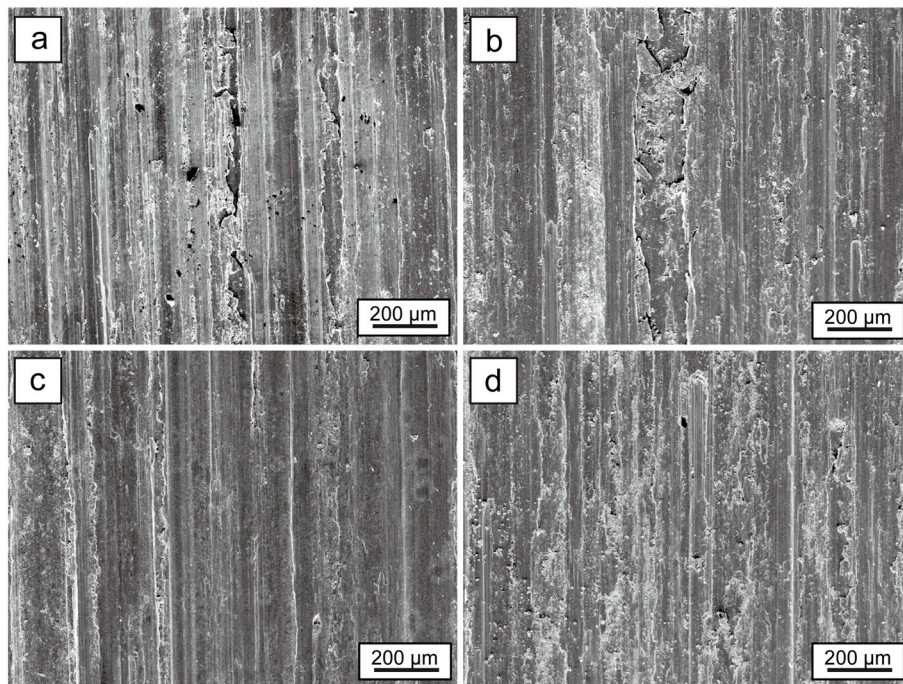**Figure 15.** The friction and wear test result of TMCs with a different inoculants content.

Figure 16. The SEM images of wear surface: (**a**) Ti6Al4V alloy; (**b**) TMCs modified with 0.2 wt % inoculant; (**c**) TMCs modified with 0.4 wt % inoculant; (**d**) TMCs modified with 0.6 wt % inoculant.

4. Conclusions

(1)　In situ Ti_5Si_3/Ti composite ribbons with a unique cellular structure (low regions in the center and Si-rich regions at the edge) were successfully prepared by an arc-melting and melt-spinning method.

(2)　The in situ Ti_5Si_3/Ti composite ribbon used in a Ti6Al4V melt shows a significant grain refining effect within a range of 0.2 wt % to 0.6 wt %. The refining effect is improved as the content of inoculant increases. The grain refining effect depends on sizes, weight fraction, and distribution of the Ti_5Si_3 as the effective components of inoculants for heterogeneous nucleation during the solidification process of Ti6Al4V.

(3)　The mechanical properties of the TMCs have been improved by adding a small quantity of Ti_5Si_3/Ti ribbon inoculant. The tensile properties of TMCs reached a peak of 1105 MPa with an amount of 0.4 wt % of inoculant. However, when adding a fraction of 0.6 wt %, the TMCs show the highest hardness, and best impact and wear-resisting properties.

(4)　The nano-scale Ti_5Si_3 particles with an average size of less than 10 nm are distributed homogeneously in the TMCs matrix and act as effective heterogeneous nucleation cores, which result in the significant grain refining effect on the as cast microstructure of Ti6Al4V. At the same time, the nano-Ti_5Si_3 particles act as a reinforcement in the TMC matrix that makes a contribution to the improvement of mechanical properties by dispersion strengthening as well as fine-grain strengthening.

(5)　The TMCs prepared by adding in situ Ti_5Si_3/Ti composite inoculant to a Ti6Al4V matrix show better mechanical properties than the TMCs prepared via in situ reaction directly, which is attributed to the nano-scale Ti_5Si_3 reinforcement particles distributed inside grains of the Ti6Al4V matrix homogeneously rather than being segregated at grain boundaries. It is indicated that refining and reinforcing TMCs by adding in situ Ti_5Si_3/Ti composite inoculant is an efficient method.

Author Contributions: Nuo Li and Chunxiang Cui conceived and designed the experiments; Nuo Li performed the experiments and wrote the original manuscript; Chunxiang Cui revised the manuscript and suggested improvements to the manuscript; Shuangjin Liu, Shuiqing Liu, Sen Cui, and Qian Wang contributed reagents/materials/analysis tools.

Conflicts of Interest: The authors declare no conflict of interest.

References

1. Greer, A.L. Grain refinement of alloys by inoculation of melt. *Philos. Trans. R. Soc. Lond. A* **2003**, *361*, 479–495. [CrossRef]

2. Murty, B.S.; Kori, S.A.; Chakraborty, M. Grain refinement of aluminum and its alloys by heterogeneous nucleation and alloying. *Int. Mater. Rev.* **2002**, *47*, 3–29. [CrossRef]

3. Liu, S.Q.; Wang, X.; Cui, C.X.; Zhao, L.C.; Liu, S.J.; Chen, C. Fabrication, microstructure and refining mechanism of in situ CeB_6/Al inoculants in aluminum. *Mater. Des.* **2013**, *65*, 432–437. [CrossRef]

4. Wang, K.; Cui, C.X.; Wang, Q.; Qi, Y.M.; Wang, C. Fabrication of in situ AlN–Al inoculants and its refining efficiency and reinforcing effect on pure aluminum. *J. Alloys Compd.* **2013**, *547*, 5–10. [CrossRef]

5. Liu, S.Q.; Wang, X.; Cui, C.X.; Zhao, L.C.; Li, N.; Zhang, Z.; Ding, J.H. Enhanced grain refinement of in situ CeB_6/Al composite inoculant on pore aluminum by microstructure control. *J. Alloys Compd.* **2017**, *701*, 926–934. [CrossRef]

6. Qiu, D.; Zhang, M.X.; Talor, J.A.; Kelly, P.M. A new approach to designing a grain refiner for Mg casting alloy and its use in Mg–Y—Based alloy. *Acta Mater.* **2009**, *57*, 3052–3059. [CrossRef]

7. Mallaiah, G.; Kumar, A.; Reddy, P.R.; Reddy, G.M. Influence of grain refining elements on mechanical properties of AISI 430 ferritic stainless steel weldments—Taguchi approach. *Mater. Des.* **2012**, *36*, 443–450. [CrossRef]

8. Banerji, A.; Reif, W. Grain refining of aluminum by TiC. *Metall. Trans. A* **1985**, *16*, 2065–2068. [CrossRef]

9. Huang, L.J.; Geng, L.; Xu, H.Y.; Peng, H.X. In situ TiC particles Ti6Al4V matrix composite reinforced with a network reinforcement architecture. *Mater. Sci. Eng. A* **2011**, *528*, 2859–2862. [CrossRef]

10. Song, M. Effects of volume fraction of SiC particles on mechanical properties of SiC/Al composites. *Trans. Nonferr. Met. Soc. China* **2009**, *19*, 1400–1404. [CrossRef]

11. Shu, S.L.; Xing, B.; Qiu, F.; Jin, S.B.; Jing, Q.C. Comparative study of the compression properties of TiAl matrix composites reinforced with nano-TiB_2 and nano-Ti_5Si_3 particles. *Mater. Sci. Eng. A* **2013**, *560*, 596–600. [CrossRef]

12. Emamy, M.; Mahta, M.; Rasizadeh, J. Formation of TiB_2 particles during dissolution of $TiAl_3$ in Al–TiB_2 metal matrix composite using an in situ technique. *Compos. Sci. Technol.* **2006**, *66*, 1063–1066. [CrossRef]

13. Cui, C.X.; Hu, B.M.; Zhao, L.C.; Liu, S.J. Titanium alloy production technology, market prospects and industry development. *Mater. Des.* **2011**, *32*, 1684–1691. [CrossRef]

14. Cui, C.X.; Bai, L.; Liu, S.J.; Qi, Y.M.; Zhao, L.C. Ti_5Si_3/β–Ti nano-core-shell structure toughened glassy Ti alloy matrix biocomposites. *RSC Adv.* **2015**, *5*, 8355–8361. [CrossRef]

15. Makoto, Y. An overview on the development of titanium alloy for non-aerospace in Japan. *Mater. Sci. Eng. A* **1996**, *213*, 8–15.

16. Boyer, R.R. An over on the use of titanium in the aerospace industry. *Mater. Sci. Eng. A* **1996**, *213*, 103–114. [CrossRef]

17. Li, N. Fabrication of the Ti_5Si_3/Ti composite inoculants and its refining mechanism on pure titanium. *Met. Mater. Int.* **2017**, *23*, 397–404. [CrossRef]

18. Zhao, L.; Cui, C.X.; Liu, S.J.; Zhao, L.C.; Li, N. Microstructure and mechanical propertied of TC4 alloy modified and reinforced by TiB+TiN/Ti inoculants ribbons. *Mater. Sci. Eng. A* **2016**, *663*, 8–16. [CrossRef]

19. Rahoma, H.K.S.; Chen, Y.Y.; Wang, X.P.; Xiao, S.L. Influence of (TiC + TiB) on the microstructure and tensile properties of Ti–B20 matrix alloy. *J. Alloys Compd.* **2015**, *627*, 415–422. [CrossRef]

20. Liu, Y.B.; Liu, Y.; Tang, H.P.; Wang, B.; Liu, B. Fabrication and mechanical properties of in situ TiC/Ti metal matrix composites. *J. Alloys Compd.* **2011**, *509*, 3592–3601.

21. Li, C.L.; Zhan, Y.Z.; Mo, Y.F.; She, Y. In situ synthesized Ti_5Si_3/Ti–Mo lightweight structural composites. *Int. J. Refract. Met. Hard Mater.* **2013**, *41*, 432–436. [CrossRef]

22. Buaanova, M.; Tretyachenko, L.; Meleshevich, K.; Vereshchaka, V.; Galadzhyj, O.; Kulak, L.; Firstov, S. Influence of tin on the structure and properties of as-cast Ti-rich Ti–Si alloys. *J. Alloys Compd.* **2003**, *350*, 164–173. [CrossRef]

23. Wei, Z.J.; Cao, L.; Wang, H.W.; Zou, C.M.; Cao, L. Microstructure and mechanical properties of TiC/Ti–6Al–4V composites processed by in situ casting route. *J. Mater. Sci. Technol.* **2011**, *27*, 1321–1327. [CrossRef]

24. Ma, F.C.; Lu, W.J.; Qin, J.N.; Zhang, D. Strengthening mechanisms of carbon element in in situ TiC/Ti–1100 composites. *J. Mater. Sci.* **2006**, *41*, 5395–5398. [CrossRef]

25. Liu, S.Q.; Cui, C.X.; Wang, X.; Li, N.; Shi, J.J.; Cui, S.; Chen, P. Effect of cooling rate on microstructure and grain refining behavior of in situ CeB_6/Al composite inoculant in aluminum. *Metals* **2017**, *7*, 204. [CrossRef]

26. Sjöberg, L.E. A general model for modifying Stokes' formula and its least-squares solution. *J. Geod.* **2003**, *77*, 459–464. [CrossRef]

27. Bramfittt, B.L. The effect of carbide and nitride additions on the heterogeneous nucleation behavior of liquid iron. *Metall. Mater. Trans.* **1970**, *1*, 1987–1995. [CrossRef]

28. Cui, C.X.; Li, Y.C.; Wu, R.J.; Greer, A.L. Particle-matrix interface microstructure of in site TiCp–AlNp/Al composite. *Compos. Sci. Technol.* **2012**, *72*, 1423–1429. [CrossRef]